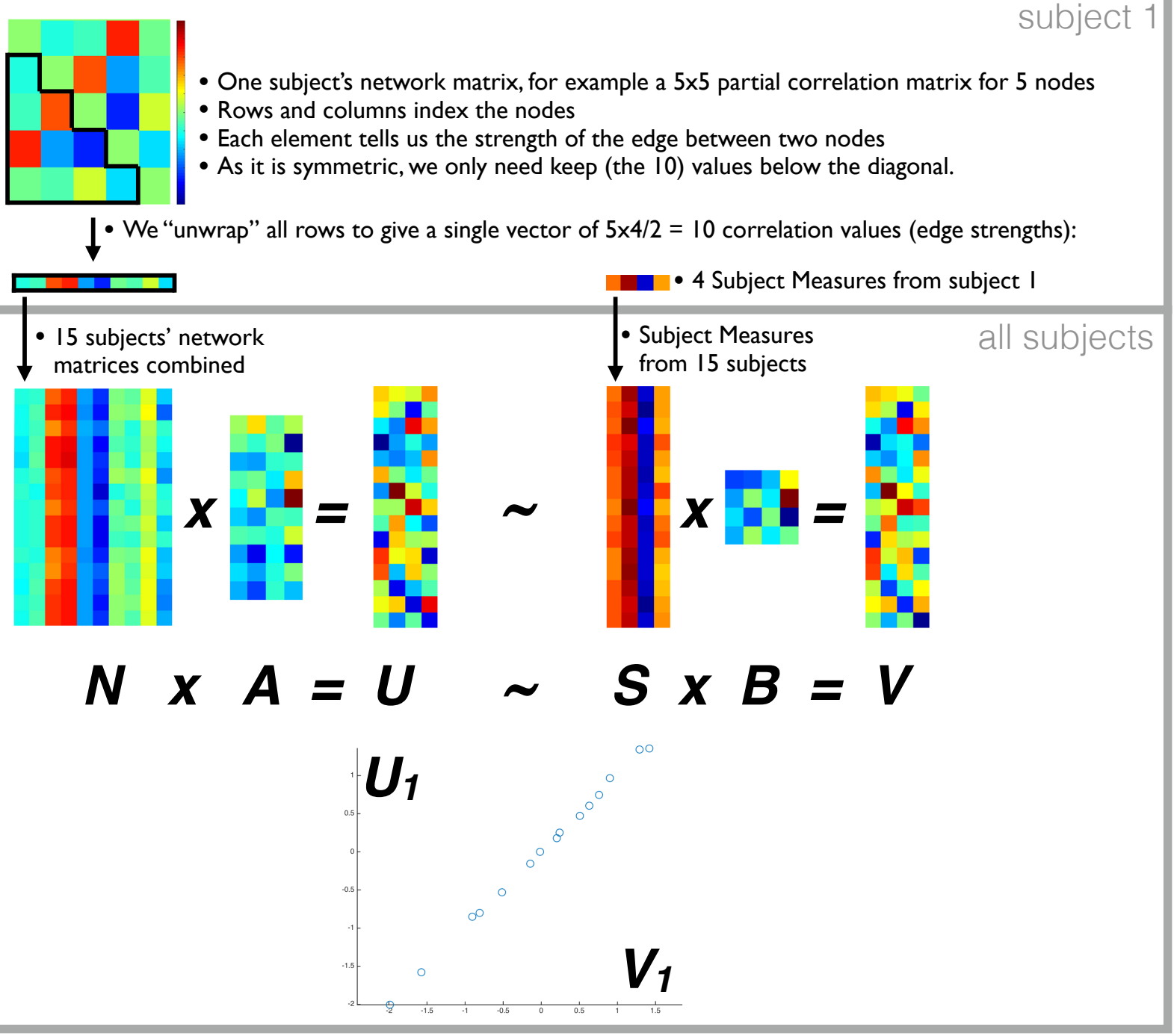

Supplementary Figure 1 Illustration of the CCA-based analysis. For a given subject, the network matrix is estimated. This is the functional connectome – in this simplified example using just 5 nodes or brain regions. This 5x5 partial correlation matrix is estimated by regressing the node spatial maps into the resting-state timeseries data – i.e., is similar to averaging the timeseries within each of the 5 nodes. Rows and columns index the nodes, and each matrix element reflects the strength of the edge between two nodes. As the network matrix is symmetric, we only need keep (the 10) values below the diagonal. These are unwrapped to form a long row vector that can then be combined with the unwrapped connectomes from all other subjects, forming matrix *N* (all connectomes from all subjects). Similarly, all subject measures from all subjects are combined into a single matrix *S*. These are fed into CCA, which estimates unmixing matrices *A* and *B* in order to find latent modes of population variation (*U* and *V*) which correlate most highly with each other. These are sorted such that the correlation between a column in *U* and the corresponding column in *V* decreases with increasing CCA mode number (column number). For a given CCA mode, the values in a pair of columns in *U* and *V* reflect the weights describing the extent to which that mode is present in a given subject (typically positive or negative, relative to the population average). Similarly, the corresponding column in *A* describes the extent to which that mode (of population co-variation) is found in a given connectome edge, and the column in *B* describes the extent to which that mode is present in a given subject measure. (In practice, each column in *N* and *S* would have its mean subtracted before being fed into CCA.)

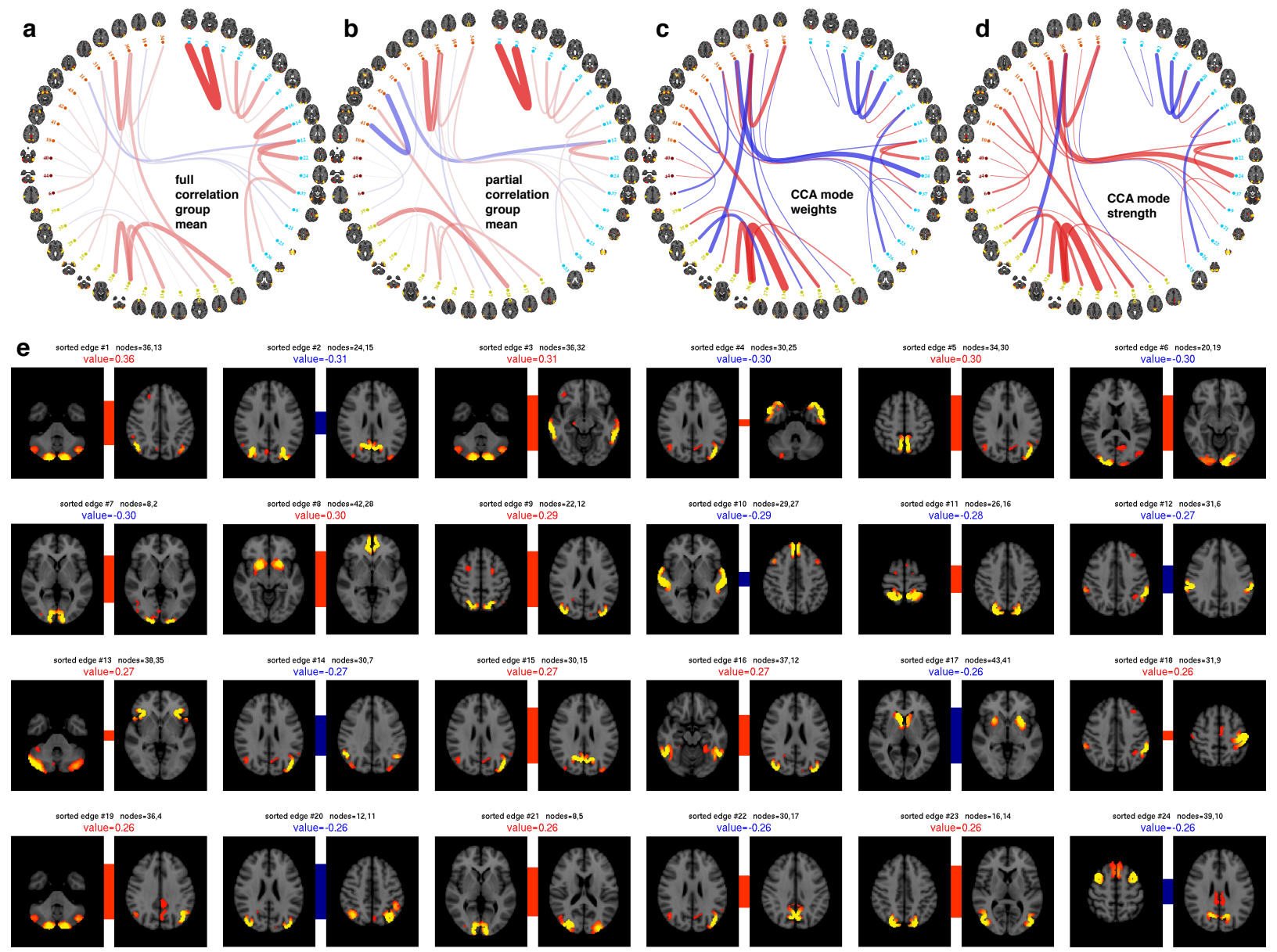

Supplementary Figure 2 The CCA mode connection strength weights. These strengths are seen in **(d)** (as shown also in **Fig. 2**), alongside the population-mean full correlation connections **(a)**, population-mean partial correlation connections **(b)** and CCA mode connection weights without multiplication by the sign of the mean connection **(c)**. Whereas (almost by definition) the within-cluster correlations are almost entirely positive **(a)**, the CCA modulations of these are both positive and negative **(c)**. The connections shown are the 30 most highly CCA-modulated edges. Also shown are the 24 connections (between node-pairs) with the strongest CCA weights **(e)** – the same information that drives the plots shown in the top row. The colored bars depict the strength and sign of the population-mean connectivity (partial correlation), and the colored text "values" are the CCA mode weights of population connectivity modulation. The most strongly modulated brain connection is that between the temporo-parietal junction and the cerebellum (correlation of 0.36 between the CCA mode and the connectomes).

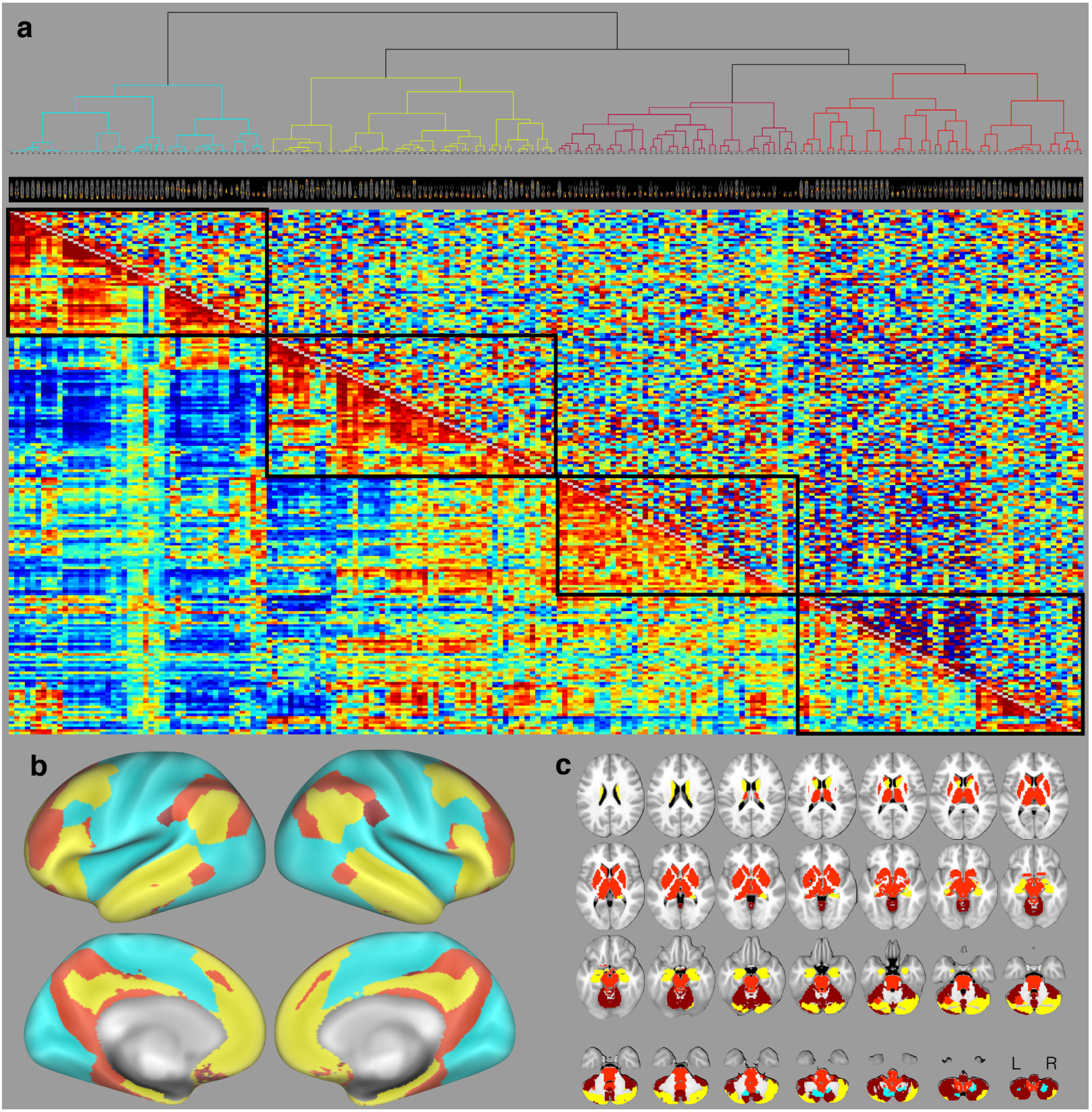

Supplementary Figure 3 Population-average connectivity and node clustering. **(a)** The nodesXnodes population average full-correlation connectivity (below the diagonal) and the population average partial-correlation connectivity (above the diagonal). For this display, the nodes are ordered according to a hierarchical clustering driven by the full correlation, therefore bringing together groups of nodes with the strongest similarity between their resting-state timeseries. Four major gross clusters are identified **(b,c)**: 1) one cluster (blue) relates to sensory, motor and dorsal attention network ("task positive network") areas[6]; the other dominant cortical cluster (yellow) identifies the default mode network[6,7], and the two others (brown and red) relate to extended/secondary default-mode areas and subcortical/cerebellar areas. At an even simpler level of clustering, these form into two groups: the sensory/motor/dorsal-attention cluster (blue) and default-mode/extended-default-mode/subcortical (warm colors).

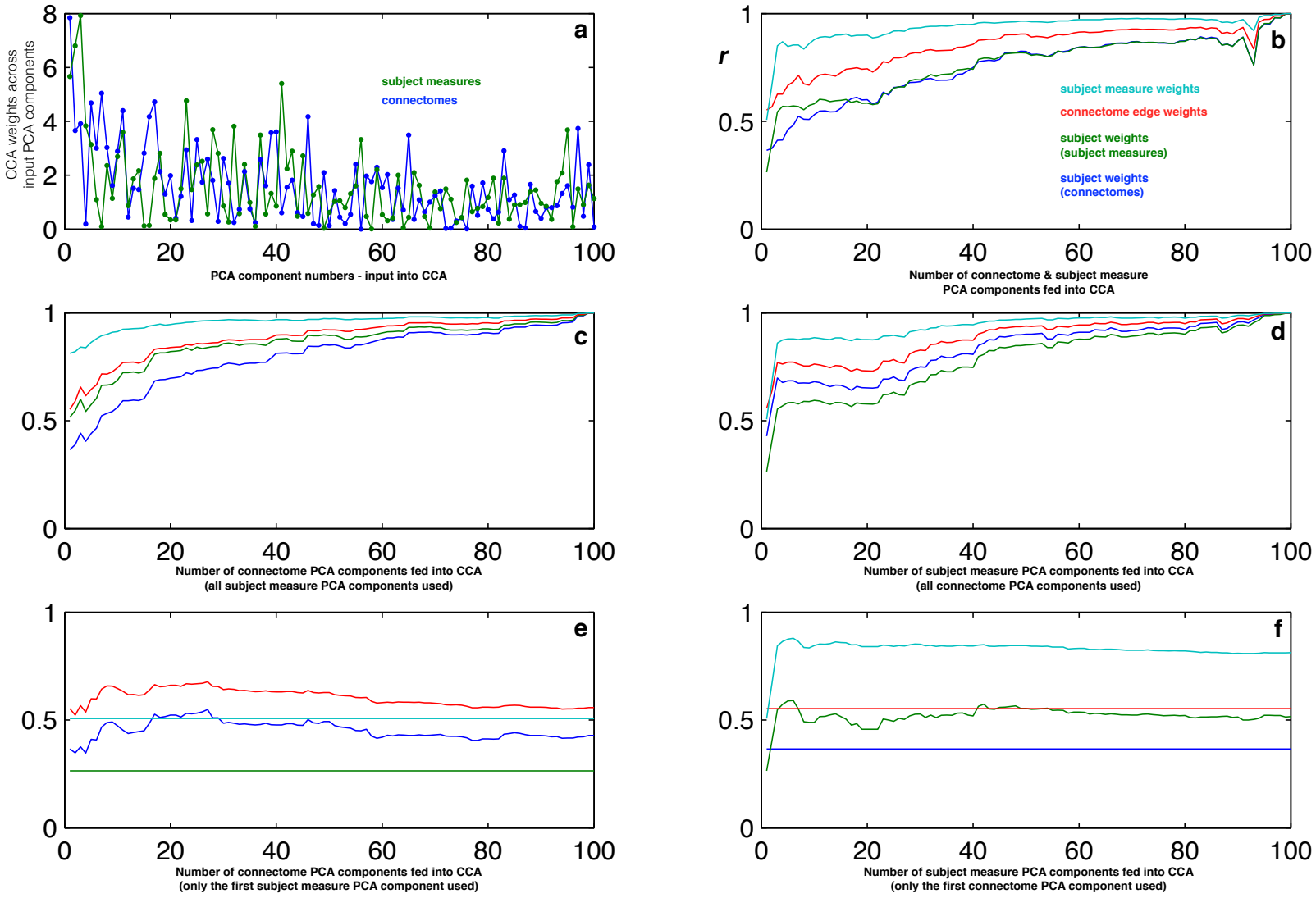

Supplementary Figure 4 Plots showing relationships between the SM and connectome PCA components to the main CCA mode. In our primary analysis, the connectome and subject measure matrices were each (separately) reduced to their top 100 PCA components, which were then fed into the CCA. **(a)** shows the CCA weights associated with the 100 PCA components, separately for connectomes and SMs. Although the first few PCA components have stronger weights than later components, the reduction in weight strengths over the PCA components is not large, suggesting that the main CCA mode is not simply reflecting the primary mode of population variation in the connectomes or the (separately estimated) primary mode of variation in the subject measures. Indeed, the weights for the second and third SM PCA components are *higher* than for the first. However, it is difficult to tell from this plot whether the higher-numbered PCA component weights are primarily reflecting noise, and hence the other plots in this figure are more informative on that issue. **(b)** shows the extent to which various CCA outputs are similar to the original result when a smaller number of PCA components is fed into CCA; the connectome edge weights (for the first CCA component) are correlated with the equivalent set of weights from the main analysis, and similar calculations are made for the subject measure weights, as well as the subject weights (from matrices *U* and *V*). The CCA results remain quite similar to the original result, as the number of PCA components fed in is gradually reduced by a reasonable number. **(c-f)** investigate this question in more detail, again leading to the conclusion that *multiple* within-connectome and within subject measure PCA modes are required in order to obtain the CCA result.

r	%var	SM
0.41	17	PicVocab_Unadj
0.39	16	PicVocab_AgeAdj
0.38	14	PMAT24_A_CR
0.38	12	DDisc_AUC_200
0.36	14	SSAGA_Educ
0.36	12	DDisc_SV_1yr_200
0.35	11	DDisc_SV_6mo_200
0.34	8	DDisc_SV_3yr_200
0.34	12	LifeSatisf_Unadj
0.34	9	DDisc_SV_5yr_200
0.34	11	ListSort_AgeAdj
0.33	11	ReadEng_Unadj
0.33	10	SCPT_TN
0.33	10	SCPT_SPEC
0.33	12	ReadEng_AgeAdj
0.33	11	ListSort_Unadj
0.32	10	DDisc_AUC_40K
0.31	6	DDisc_SV_10yr_200
0.31	11	DDisc_SV_5yr_40K
0.30	9	PicSeq_AgeAdj
0.29	8	SSAGA_TB_Yrs_Since_Quit
0.29	8	PicSeq_Unadj
0.28	8	DDisc_SV_3yr_40K
0.28	9	DDisc_SV_1yr_40K
0.27	8	SSAGA_Income
0.27	7	Dexterity_AgeAdj
0.27	6	DDisc_SV_10yr_40K
0.26	7	Dexterity_Unadj
0.25	5	DDisc_SV_6mo_40K
0.24	6	DDisc_SV_1mo_200
0.22	5	FamHist_Fath_None
0.22	5	ProcSpeed_AgeAdj
0.22	4	Endurance_AgeAdj
0.21	4	Endurance_Unadj
0.20	4	DDisc_SV_1mo_40K
-0.21	4	SSAGA_TB_Age_1st_Cig
-0.21	3	ASR_Rule_Pct
-0.22	6	ASR_Thot_Raw
-0.22	4	EVA_Denom
-0.22	5	SSAGA_TB_Still_Smoking
-0.22	5	ASR_Thot_Pct
-0.22	4	PercStress_Unadj
-0.23	5	Taste_AgeAdj
-0.23	4	ASR_Rule_Raw
-0.23	5	Taste_Unadj
-0.24	6	AngAggr_Unadj
-0.25	6	Times_Used_Any_Tobacco_Today
-0.25	6	PSQI_Score
-0.26	6	Avg_Weekend_Cigarettes_7days
-0.28	7	Avg_Weekend_Any_Tobacco_7days
-0.28	6	Total_Cigarettes_7days
-0.29	6	Avg_Weekday_Cigarettes_7days
-0.30	9	FamHist_Fath_DrgAlc
-0.31	9	Num_Days_Used_Any_Tobacco_7days
-0.31	7	Total_Any_Tobacco_7days
-0.32	7	Avg_Weekday_Any_Tobacco_7days
-0.33	10	SCPT_FP
-0.35	12	THC
-0.36	12	PMAT24_A_SI

included in CCA
excluded

Supplementary Table 1 The full set of SMs (subject measures) most strongly associated with the CCA mode of population variability (abs(*r*)>0.2 ; because of the multivariate nature of the CCA, we can estimate p-values for a complete mode, but not for individual elements of it). Whereas in **Fig. 1** we listed SMs according to descriptive free-form text, here we show the SMs using the formal variable names as defined at wiki.humanconnectome.org/display/PublicData/HCP+Data+Dictionary+Public-+500+Subject+Release (the HCP Data Dictionary). SMs used in the CCA are colored blue, while those colored grey were not; both sets of SMs were then correlated with the CCA mode post-hoc. Vertical position is according to correlation with the CCA mode (first column), while the second column reports the percentage variance explained (of the SM by the CCA mode).

cluster	areas / networks	Neurosynth decoding: top distinct terms	Jülich Cytoarchitectonic Map Areas (area names & overlap with 50% probability mask in mm^3)
1 brown	cerebellum, inferior parietal lobule A / Brodmann 40	cerebellum	Cerebellum_IX_Hem 3497, Cerebellum_IX_Verm 280, Cerebellum_I_IV_Hem 2550, Cerebellum_VIIIa_Hem 9238, Cerebellum_VIIIa_Verm 1982, Cerebellum_VIIIb_Hem 8306, Cerebellum_VIIIb_Verm 786, Cerebellum_VIIa_crusII_Hem 5092, Cerebellum_VIIa_crusII_Verm 393, Cerebellum_VIIa_crusI_Hem 11629, Cerebellum_VIIb_Hem 7763, Cerebellum_VIIb_Verm 317, Cerebellum_VI_Hem 22621, Cerebellum_VI_Verm 2063, Cerebellum_V_Hem 8784, Cerebellum_X_Hem 219, IPL_PF 450, IPL_PFcm 14, IPL_PFt 80, Visual_FG1 186, Visual_FG2 113, Visual_hOc3v 98, Visual_hOc4v 132
2 red	extended/secondary default mode network, subcortex, brainstem nuclei	brainstem, thalamus, subcortical, dopaminergic, reward, anticipation	AIPS_IP1 873, AIPS_IP2 294, AIPS_IP3 395, Broca_45 67, Cerebellum_IX_Hem 4279, Cerebellum_IX_Verm 626, Cerebellum_I_IV_Hem 1866, Cerebellum_VIIIb_Hem 28, Cerebellum_VIIa_crusI_Hem 299, Cerebellum_VI_Hem 235, Cerebellum_X_Hem 33, Cerebellum_X_Verm 190, Cingulum_25 15, Cingulum_33 21, Cingulum_s24 13, FrontalPole_Fp1 3429, Hippocampus_DG 176, Hippocampus_Subc 213, IPL_PF 1326, IPL_PFm 870, IPL_PFt 141, IPL_PGa 89, IPL_PGp 2420, SPL_7A 70, SPL_7P 233, wThalamus_Motor 352, wThalamus_Parietal 1653, wThalamus_Prefrontal 5958, wThalamus_Premotor 995, wThalamus_Somatosensory 335, wThalamus_Temporal 1314, wThalamus_Visual 196
3 yellow	default mode network	cerebellum, theory of mind, autobiographical, mentalizing, comprehension, default mode	Amygdala_LB 1095, Amygdala_SF 118, Auditory_Te3 437, Broca_44 1041, Broca_45 2325, Cerebellum_VIIa_crusII_Hem 14765, Cerebellum_VIIa_crusII_Verm 151, Cerebellum_VIIa_crusI_Hem 27642, Cerebellum_VIIb_Hem 598, Cerebellum_VI_Hem 1952, Cerebellum_VI_Verm 83, FrontalPole_Fp1 11132, FrontalPole_Fp2 3958, Hippocampus_CA1 1509, Hippocampus_CA2 62, Hippocampus_CA3 111, Hippocampus_DG 308, Hippocampus_EC 95, Hippocampus_HATA 25, Hippocampus_Subc 1480, IPL_PF 597, IPL_PFm 1452, IPL_PGa 2141, IPL_PGp 693, Visual_FG2 92, Visual_hOc4v 52, wThalamus_Prefrontal 15
4 blue	sensory, motor, dorsal attention network	primary visual, objects, visual motion, face, sensorimotor	AIPS_IP2 22, AIPS_IP3 870, Auditory_Te10 257, Auditory_Te11 38, Auditory_Te12 30, Auditory_Te3 1997, Broca_44 1553, Cerebellum_IX_Hem 250, Cerebellum_VIIIa_Hem 1079, Cerebellum_VIIIb_Hem 137, Cerebellum_VIIIb_Verm 32, Cerebellum_VIIa_crusI_Hem 16, Cerebellum_VIIb_Hem 165, Cerebellum_VI_Hem 57, IPL_PF 615, IPL_PFcm 26, IPL_PFop 539, IPL_PFt 2646, IPL_PGp 571, Motor_4a 4697, Motor_4p 1730, Operculum_OP1 410, Operculum_OP2 58, Operculum_OP3 27, Operculum_OP4 967, PSC_1 2948, PSC_2 3887, PSC_3a 712, PSC_3b 1855, SPL_5L 2261, SPL_5M 586, SPL_7A 2229, SPL_7M 140, SPL_7P 120, SPL_7PC 690, Visual_FG1 1296, Visual_FG2 1707, Visual_hOc1 14918, Visual_hOc2 2879, Visual_hOc3d 2925, Visual_hOc3v 5071, Visual_hOc4d 1653, Visual_hOc4la 4233, Visual_hOc4lp 5365, Visual_hOc4v 4730, Visual_hOc5 285

Supplementary Table 2 Spatial mapping of 4 primary functional clusters against Neurosynth decoding terms and cytoarchitectonic areas. As shown above, the CCA mode spatially overlaps highly with clusters 1-3. Column 2 lists our terminology for the primary areas/networks covered by the clusters. Column 3 lists the main distinct terms reported by the "Decoding" function in Neurosynth (http://neurosynth.org) when fed with the cluster maps. These include both area/network names and functions associated with these areas in the literature, as automatically extracted by Neurosynth. Column 4 lists areas defined in the Jülich Cytoarchitectonic Anatomy Toolbox (v2.1: Eickhoff S, *et al. NeuroImage* 25(4), 1325-1335, 2005). Each cytoarchitectonic area is thresholded at 50% (population) probability, and the volumetric overlap in mm^3 is reported for each of the 4 clusters (where the overlap is greater than 10 mm^3).